THE ASTROPHYSICAL JOURNAL, 543:634–643, 2000 November 10

PROBING THE INTERSTELLAR MEDIUM IN EARLY-TYPE GALAXIES WITH *INFRARED SPACE OBSERVATORY* OBSERVATIONS

S. MALHOTRA,[1,2,3] D. HOLLENBACH,[4] G. HELOU,[5] N. SILBERMANN,[5] E. VALJAVEC,[5] R. H. RUBIN,[4] D. DALE,[5] D. HUNTER,[6] N. LU,[5] S. LORD,[5] H. DINERSTEIN,[7] AND H. THRONSON[8]

Received 1999 July 1; accepted 2000 June 15

ABSTRACT

Four *IRAS*-detected early-type galaxies were observed with the *Infrared Space Observatory* (*ISO*). With the exception of the 15 μm image of NGC 1052, the mid-IR images of NGC 1052, NGC 1155, NGC 5866, and NGC 6958 at 4.5, 7, and 15 μm show extended emission. Mid-IR emission from NGC 1052, NGC 1155, and NGC 6958 follows a de Vaucouleurs profile. The ratio of 15 μm/7 μm flux decreases with radius in these galaxies, approaching the values empirically observed for purely stellar systems. In NGC 5866, the 7 and 15 μm emission is concentrated in the edge-on dust lane. All the galaxies are detected in the [C II] (158 μm) line, and the S0s NGC 1155 and NGC 5866 are detected in the [O I] (63 μm) line as well. Previous detections of neutral interstellar medium (ISM) are sparse: only NGC 1052 had been detected in H I and NGC 5866 in CO. The *ISO* long-wavelength spectrograph observations of the [C II] line are more sensitive measures of cool neutral ISM than H I and CO by about a factor of 10–100. Comparison of [C II] with Hα shows that [C II] does not arise in H II regions and therefore must arise in the neutral medium. Three of four early-type galaxies, namely, NGC 1052, NGC 6958, and NGC 5866, have low ratios of far-infrared to blue luminosity and show a lower $L_{[\mathrm{C\,II}]}/L_{\mathrm{FIR}}$, which is explained by postulating a softer radiation field from old stellar populations in early-type galaxies, compared to spirals and irregulars, where young stars are present. While optical photons are effective in heating the dust, UV radiation is needed to heat the gas by the grain photoelectric mechanism. The low [C II]/CO ratio in NGC 5866 [$L_{[\mathrm{C\,II}]}/L_{\mathrm{CO}}(1\text{–}0) \leq 570$] confirms this scenario. We estimate the UV radiation expected from the old stellar populations in these galaxies and compare it to that needed to heat the gas to account for the cooling observed [C II] and [O I] lines. In three out of four galaxies, NGC 1052, NGC 5866, and NGC 6958, the predicted UV radiation falls short by a factor of 2–3 of that required to sufficiently heat the gas. In view of the observed intrinsic scatter in the "UV upturn" in elliptical galaxies and its great sensitivity to age and metallicity effects, this difference is not significant. However, the much larger difference (about a factor of 20) between the UV radiation from old stars and that needed to produce the far-infrared lines for NGC 1155 is strong evidence for the presence of an additional UV source, probably young stars, in NGC 1155.

Subject headings: galaxies: elliptical and lenticular, cD — galaxies: ISM — infrared: ISM: continuum — infrared: ISM: lines and bands — ISM: atoms — radiation mechanisms: thermal

1. INTRODUCTION

A significant fraction of early-type galaxies (ellipticals and S0s) contain some cool interstellar medium (ISM) including neutral gas and dust (Jura et al. 1987; Knapp et al. 1989). However, the physical conditions in the ISM in these galaxies are relatively unknown. Many ellipticals have been detected by the X-ray emission of hot gas (Roberts et al. 1991) and many in the H I and CO lines indicating cold neutral medium (Lees et al. 1991; Wiklind, Combes, & Henkel 1995) and through dust obscuration (Sadler & Gerhard 1985; Goudfrooij et al. 1994a, 1994b). The environment in the ellipticals may lead to different equilibrium physical conditions in the various phases of the ISM because of the presence of hot X-ray gas and a higher ratio of stellar radiation compared to the cool gas and dust. But the *IRAS* colors in 60 and 100 μm emission indicate cold dust with temperatures comparable to those found in spirals.

We observed four elliptical/S0 galaxies with the *Infrared Space Observatory* (*ISO*) (Kessler et al. 1996) to study the physical conditions in the gas and dust in these galaxies. These galaxies are part of a large sample of normal star-forming galaxies spanning a range of morphologies, infrared luminosities, far-infrared (FIR) colors [$F_\nu(60)/F_\nu(100)$] and FIR-to-blue ratio. ISOCAM (Cesarsky et al. 1996) images at 7 and 15 μm are used to determine the distribution of mid-IR emission (§ 3) and hence its origin. The mid-IR spectrum of NGC 5866 was taken with ISOPHT (Lemke et al. 1996) and is presented by Lu et al. (2000, in preparation). The FIR spectroscopy of fine-structure lines [C II] (158 μm) and [O I] (63 μm) was carried out with the *ISO* long-wavelength spectrograph (LWS) (Clegg et al. 1996). Assuming [C II] and [O I] to be the major cooling lines, we estimate gas-heating rates and examine possible heat sources in these galaxies in § 4. For NGC 1155 and NGC 5866 where both [C II] (158 μm) and [O I] (63 μm) lines were detected, we estimate the radiation and gas density, G_0 and n.

[1] Postal address: Kitt Peak National Observatory, P.O. Box 26732, Tucson, AZ 85705.
[2] Hubble Fellow.
[3] Now at Johns Hopkins University, Baltimore, MD 21218.
[4] NASA/Ames Research Center, MS 245-3, Moffett Field, CA 94035.
[5] IPAC, 100-22, California Institute of Technology, Pasadena, CA 91125.
[6] Lowell Observatory, 1400 Mars Hill Road, Flagstaff, AZ 86001.
[7] University of Texas, Astronomy Department, RLM 15.308, Austin, TX 78712.
[8] NASA Headquarters.

The sample considered in this paper consists of two elliptical galaxies (NGC 6958 and NGC 1052) and two S0 galaxies (NGC 1155 and NGC 5866). Like any sample of four galaxies, these have varied properties. NGC 1052 harbors an active nucleus (Fosbury et al. 1978). NGC 5866 has a large edge-on disk. NGC 1155 is labeled an elliptical in the NASA/IPAC Extragalactic Database (NED) but has been reclassified as an S0 by Dale et al. (2000) based on morphology using *B*-band CCD images taken at Lowell Observatory. These images were taken with a CCD camera with 0.″61 pixels and approximately 1.″5 seeing. This galaxy is small (0.′8) and distant which may make a definitive classification difficult. The *B*-band surface brightness profile is well fit by a de Vaucouleurs profile and cannot be fit with a point source plus exponential disk. NGC 1155 is also labeled a starburst in NED and is a Markarian galaxy. It has a spiral companion (NGC 1154) 2′ away, and a bridge can be seen between the two galaxies in deep optical images. NGC 6958 seems the most unremarkable galaxy in this set.

2. OBSERVATIONS AND DATA ANALYSIS

The mid-IR imaging of NGC 1155 and NGC 6958 was done with ISOCAM at 6.75 μm (LW2 filter, $\Delta\lambda = 3.5$ μm) and at 15 μm (LW3 filter, $\Delta\lambda = 6$ μm) using the raster scan mode to cover roughly 4.′5 × 4.′5 centered on the nucleus. CAM was set to 6″ pixel^{-1}, and the raster was made up of 2 × 2 pointings separated by 81″, or 13.5 pixels in each direction, allowing for better spatial sampling. At each pointing in the raster scan, we integrated for 50 s in each band: 25 × 2 s exposures at 15 μm and 10 × 5 s at 7 μm. Typical sensitivity is 0.02 Jy pixel^{-1} in the 7 μm filter and 0.04 Jy pixel^{-1} in the 15 μm filter. More details of CAM data reduction can be found in Dale et al. (2000). NGC 1052 and NGC 5866 were observed by Vigroux et al. (1999) in the LW1 (4.5 μm), LW2 (7 μm), and LW3 (15 μm) filters with 3″ pixel^{-1} and 6″ pixel^{-1}. A detailed analysis of these data will be presented by Madden et al. (2000, in preparation).

With the 80″ beam of the LWS and spectral resolution of 0.6–0.3 μm, we measure total line flux for these galaxies. The galaxies are estimated to have FWHM $< 0.'5$ in FIR emission using deconvolved IRAS maps. The [C II] line observations were planned to achieve (1 σ) sensitivities of $5 \times 10^{-5} \times F_{\rm FIR}$, where $F_{\rm FIR}$ is the total far-infrared flux of the galaxy and is computed according to the relation $F_{\rm FIR} = 1.26 \times 10^{-14}[2.58 \times F_\nu(60\ \mu{\rm m}) + F_\nu(100\ \mu{\rm m})]$ W m^{-2} (Helou et al. 1988), where $F_\nu(60\ \mu{\rm m})$ and $F_\nu(100\ \mu{\rm m})$ are flux densities in Janskys at 60 and 100 μm measured by *IRAS*.

The data were reduced and calibrated with the *ISO* data reduction pipeline OLP7.0. Postpipeline data reduction and recalibration was carried out using an interactive data reduction package ISAP.[9] The line profiles were derived from several scans by running a median boxcar filter through the scans. We use the median of the observed fluxes instead of the mean to reduce the influence of outlying points arising from cosmic-ray hits. Line fluxes were derived by integrating directly under the lines, after fitting a linear baseline to the continuum (cf. Malhotra et al. 2000 for details on the LWS data reduction and line fluxes).

Optical imaging of NGC 1155 was done at Lowell Observatory. The Hα images were obtained through narrowband filters centered at the line; an off-band filter was used to image and subtract the continuum. Long-slit spectroscopy and Hα and broadband imaging of NGC 1155 was done at Lowell Observatory. CO(1–0) observations on NGC 6958 were carried out at the Swedish ESO Submillimeter Telescope (SEST).

[9] Available at http://www.ipac.caltech.edu/iso/lws/lws.html.

3. MID-INFRARED IMAGING

In spiral galaxies the mid-IR emission is dominated by small grains transiently heated to high temperatures and the fluorescence of large aromatic molecules (Puget & Leger 1989). This may not be the case for ellipticals given that the ISM-to-stellar ratio is low. A significant part of the emission at 12 μm could be from photospheres and circumstellar dust (Knapp, Gunn, & Wynn-Williams 1992), although Sauvage & Thuan (1994) have argued that the *IRAS* color-color relation (Helou 1986) holds for early-type as well as for late-type galaxies indicating a similar origin from ISM. Hot dust near an active nucleus can also be a major contributor in some cases. Because of its high spatial resolution and sensitivity, CAM imaging at 7 and 15 μm can tell us about the spatial distribution of the mid-IR emission in galaxies. The interpretation is complicated by the fact that the mid-IR emission maps depend on the distribution of the dust as well as the heating sources.

The mid-IR emission is extended in at least nine out of 10 mid-IR images (Fig. 1), although many of the images look compact because the light in ellipticals is very concentrated. Comparison of curves of growth (i.e., flux enclosed in a radius) show significant difference between a point source and these galaxies (Fig. 2) except for the 15 μm image of NGC 1052.

The 4.5 μm emission from NGC 1052 is extended and traces the stellar distribution. At 7 and 15 μm NGC 1052 comes closest to being dominated by the central point source, which is an active nucleus in this case. The flux in 7 and 15 μm bands in the central 6″ radius in NGC 1052 is about 80%, compared to 88% and 80% expected for a point source in 7 and 15 μm filters with 6″ pixel scale. There is some uncertainty in the expected point-spread function (PSF) depending on the placement of the point source within a 6″ pixel. NGC 1052 was also observed in the 3″ pixel^{-1} mode on CAM which samples the PSF properly. The images with 3″ pixel^{-1} show that at 7 μm NGC 1052 is extended and at 15 μm it is consistent with being unresolved (Fig. 2). In this respect it is similar to NGC 3998 whose mid-infrared emission is dominated by the active nucleus (Knapp et al. 1996). The 7 and 15 μm emission is extended for NGC 1155, where the central 6″ accounts for only 47% and 56% of the total flux at 7 and 15 μm. In NGC 5866 the central 6″ contains 24% and 40% of the total flux in 7 and 15 μm bands. In NGC 5866 the mid-IR emission at 7 and 15 μm traces the nearly edge-on dust lane, whereas the 4.5 μm emission traces the stars (Fig. 1).

To increase the signal-to-noise ratio (S/N) in the outer parts of the galaxies, we average the emission in annuli after subtracting the background determined at radii greater than 90″. Figure 3 shows the radial profile of the surface brightness in three galaxies: NGC 1052, NGC 1155, and NGC 6958. The radial surface density profile is derived by averaging azimuthally. The error bars in surface brightness in Figure 3 are derived from the scatter in pixel brightness in a given annulus. A de Vaucouleurs radial profile provides a reasonable fit to the mid-IR surface brightness profile. The effective radius for the mid-IR emission is intermediate to

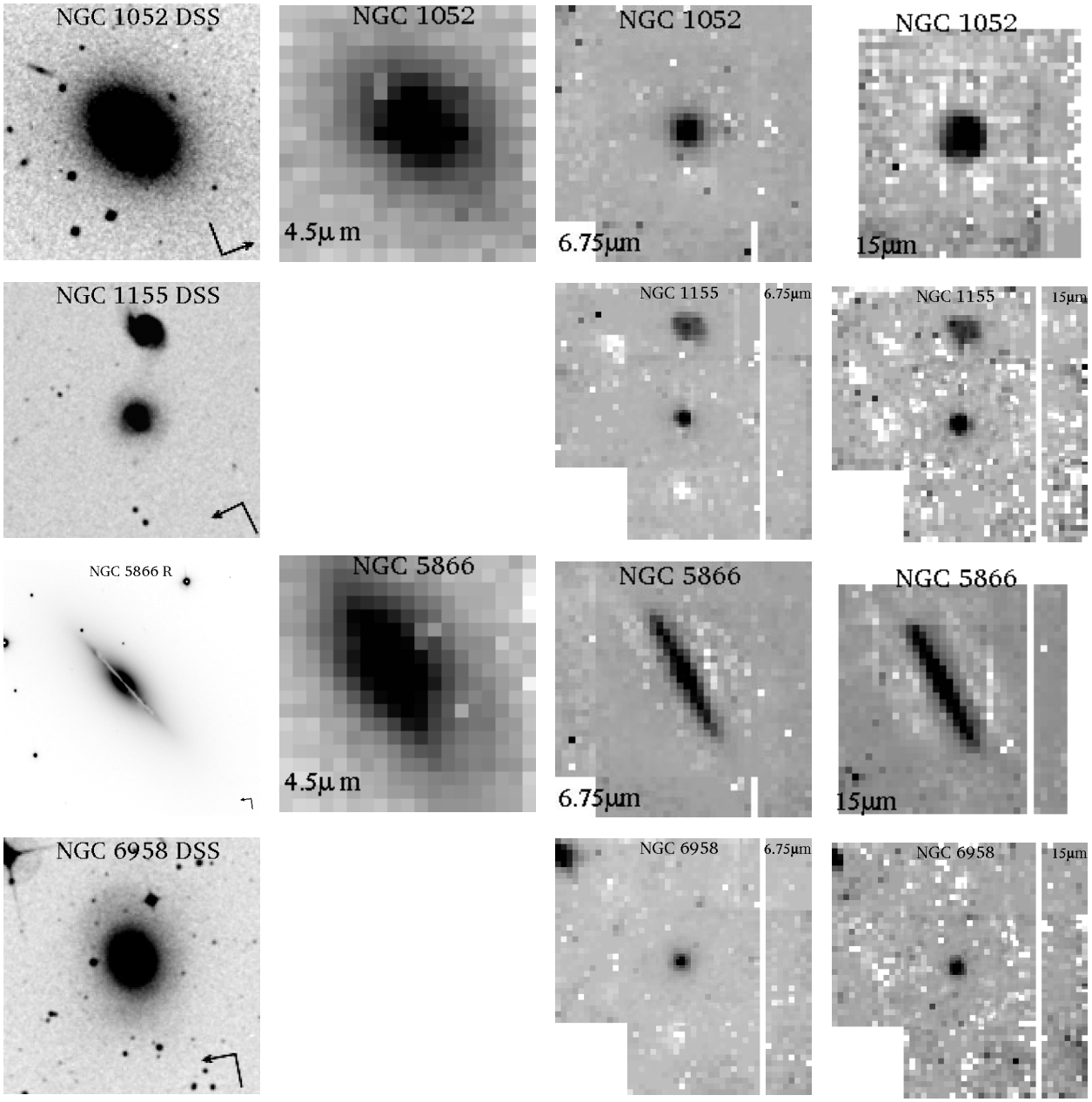

FIG. 1.—Mid-infrared and optical images of NGC 1052, NGC 1155, NGC 5866, and NGC 6958 are presented for comparison. The images are (from left to right) DSS (digitized sky survey) images in *R* and 4.5, 6.75, and 15 μm images from CAM. The 4.5 μm images of NGC 1052 and NGC 5866 trace the star light, while the 7 and 15 μm images of NGC 5866 trace the edge-on dust lane. The 7 and 15 μm images of NGC 1052 are dominated by the active nucleus. All except the 15 μm image of NGC 1052 show extended emission. The orientation of the images is indicated by the arrows on the DSS images, where the arrowhead points north. The field of view is 4.′5 on the side for NGC 1155 and NGC 6958 and 1.′5 on the side for NGC 1052 and NGC 5866.

that seen in optical *B*-band and Hα light for NGC 1155 (Fig. 4). We also note that in all three galaxies the 15 μm/7 μm ratio decreases going from the center of the galaxy outward (Fig. 3).

The 15 μm/7 μm ratio can be used as a further diagnostic to determine the origin of the mid-IR emission in the current sample. In quiescent spiral galaxies this ratio is 1 (e.g., NGC 6946; Helou et al. 1996). In more actively star-forming regions/galaxies, the 15 μm/7 μm ratio increases due to higher heating radiation (Vigroux et al. 1999; Dale et al. 1999). The ratio 15 μm/7 μm < 1 is found in early-type galaxies where the 7 μm band contains a significant contribution from stellar photospheres (Madden, Vigroux, & Sauvage 1997). In the inner parts of NGC 1052 and NGC 1155, 15 μm/7 μm is a factor $\simeq 2$ higher than the ISM in quiescent spiral galaxies (Fig. 3). This is presumably due to higher radiation density in the central regions of these galaxies due to higher density of stars or the active nucleus in the case of NGC 1052. The decrease in 15 μm/7 μm in the outer parts of the galaxy is due to different proportions of photospheric and ISM contributions, with the photospheres having a lower 15 μm/7 μm ratio (i.e., bluer emission). This scenario is consistent with the 15 μm/7 μm ratio of 0.5 seen in the outer parts of NGC 6958. This ratio is within the range of observed ratios in ellipticals devoid of ISM (Madden et al 1997), and indeed NGC 6958 does not

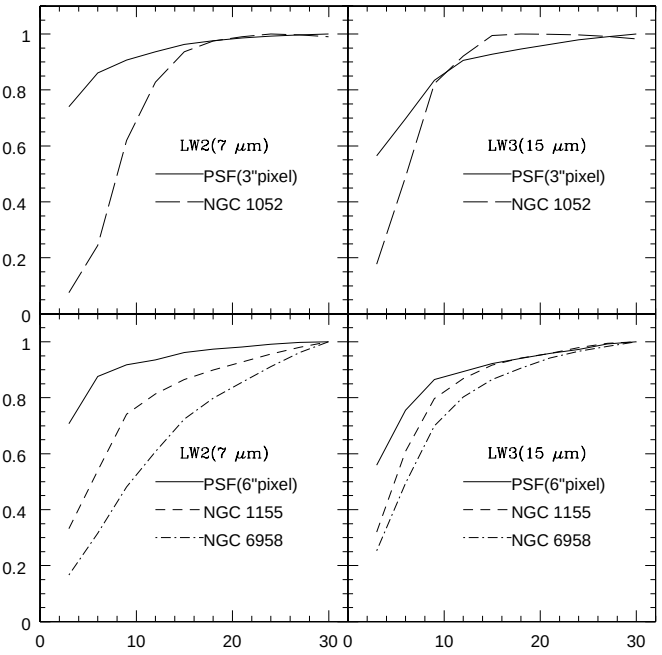

FIG. 2.—Cumulative flux profiles of elliptical galaxies at 7 and 15 μm as compared to the point-source profiles. NGC 1155 and NGC 6958 were observed in a mode with 1 pixel = 6″, and they are plotted in the lower two panels. NGC 1052 was also observed in the 3″ pixel mode, and its profile is plotted in the upper two panels. Except for the 15 μm image of NGC 1052, all other images are clearly extended. This is manifest from the slow rise of cumulative flux with radius for galaxies as compared to the point-source profile. Within measurement errors the 15 μm profile of NGC 1052 is consistent with an unresolved source.

show extended Hα emission beyond its nucleus, indicating that the ISM is not very extended in this galaxy (Phillips et al. 1986).

The spatial distribution of the mid-IR emission could also reflect the distribution of sources heating the dust. In case of NGC 1155 the mid-IR emission follows a de Vaucouleurs profile with an effective radius R_e which is intermediate between Hα and B band indicating that both ionizing and nonionizing radiation heat the dust. A similar result was found for the spiral galaxy NGC 6946 (Malhotra et al. 1996). If so, we would predict that the dust is quite extensive in NGC 1155. While the extent of the ISM is not known for NGC 1155, the luminosity in the [C II] line is as much as a third of the Milky Way value indicating the presence of a significant amount of gas. The presence of an extended component of dust can explain the discrepancy between dust masses obtained from optical extinction and FIR emission, the former being sensitive only to dust concentrated near the center (Goudfrooij et al. 1994b).

4. FAR-INFRARED SPECTROSCOPY

The physical conditions in the different phases of the ISM in early-type galaxies are not very well known, partly because there is not as much cool ISM in these galaxies and partly because we do not live in such a galaxy. Much of our detailed knowledge about the various phases of the ISM in spirals comes from being in these phases and the ability to do absorption studies. In ellipticals/S0s hot gas is detected in the X-ray, and ionized gas is detected by Hα emission. The cold neutral medium is detectable as H I (21 cm) and CO by present instrumentation for typical masses of 10^7–10^8 $M_\odot$. As a result the detection rate for cold gas is about 15%–50% (van Gorkom 1997; Rupen 1997) depending on the morphological classification of galaxies and preselection of samples. The detection rate is higher for Hα (about 50%) where one is sensitive to 10^5 $M_\odot$ of gas (Phillips et al. 1986).

The far-infrared fine-structure lines dominate the global cooling of the neutral ISM of galaxies. Of these, [C II] (158 μm) and [O I] (63 μm) are generally the strongest, with [C II] dominating the lower densities and moderate UV radiation field intensities (Hollenbach, Tielens, & Takahashi 1991; Hollenbach & Tielens 1997, 1999). We detect the [C II] transition in all four galaxies, albeit at low (3 σ) S/N for NGC 6958. The other major fine-structure cooling line, [O I] (63 μm), is detected in NGC 1155 and NGC 5866. In Table 1 we summarize what is known about the warm and cool ISM in the four early-type galaxies. Detections are few: H I (21 cm) is detected in NGC 1052 (van Gorkom et al. 1986), CO is detected in NGC 5866 (Thronson et al. 1989), and Hα is detected in all four. There is tentative detection of CO in absorption against the nucleus in NGC 1052 (Knapp & Rupen 1996). In Table 1 $M_{\rm H}(C^+)$ is the minimum mass of the hydrogen associated with the observed C^+ emission and is derived in the high-density, high-temperature limit ($n_{\rm H} > 3000$, $T \gg 91$ K), assuming solar abundance of carbon with all the carbon in the form of C^+ (Crawford et al. 1985). The value of $M_{\rm H}(C^+)$ is typically 10–100 times smaller than the observed detection or upper limits on H I and H_2.

TABLE 1

MASS IN INTERSTELLAR COMPONENTS

Name	Morphology[a]	Distance (Mpc)	M(H I) ($M_\odot$)	$M(H_2)$ ($M_\odot$)	M(H II) ($M_\odot$)	$M_{\rm H}(C^+)$	$M_{\rm dust}$[b]
NGC 1052.....	E4	14	0.7×10^{7}[c]	$<3 \times 10^{7}$[d]	3×10^{4}[e]	$>4 \times 10^{5}$	4.8×10^{4}
NGC 1155.....	S0	45	?	?	?	$>1 \times 10^{7}$	1.8×10^{6}
NGC 5866.....	S0	11.4	$<3 \times 10^{7}$[f]	$>3 \times 10^{8}$[g]	4×10^{4}[h]	$>9.7 \times 10^{5}$	1.2×10^{6}
NGC 6958.....	E+	28	$<3 \times 10^{8}$[i]	$<9 \times 10^{8}$[j]	?	$>8 \times 10^{5}$	3.5×10^{5}

[a] From NASA /IPAC Extragalactic Database and Dale et al. 2000.
[b] Roberts et al. 1991, adjusted for the given distances.
[c] From van Gorkom et al. 1986, adjusted to the LWS beam size of 70″.
[d] Knapp & Rupen 1996; Wiklind et al. 1995.
[e] Plana & Boulesteix 1996.
[f] Haynes et al. 1990.
[g] Thronson et al. 1989.
[h] Plana et al. 1998.
[i] Walsh et al. 1990.
[j] Recent observations at SEST.

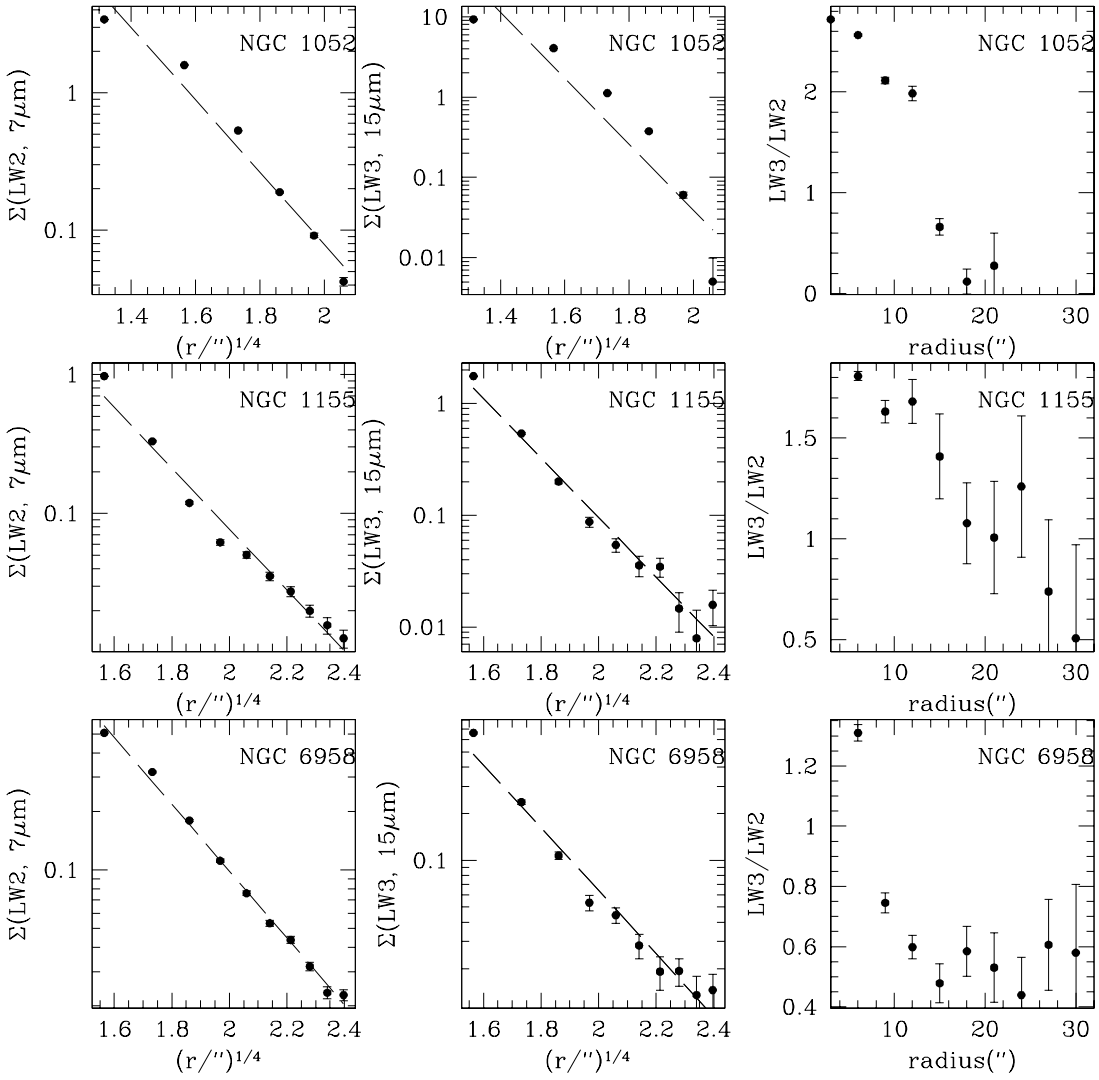

FIG. 3.—Surface brightness of early-type galaxies in the mid-infrared at 7 and 15 μm follows de Vaucouleurs radial profiles (*left and middle columns*). The ratio of LW3 (15 μm) and LW2 (7 μm) light decreases toward the outer parts of galaxies (*right column*). The 15 μm/7 μm ratio for NGC 6958 reaches an asymptotic value of 0.5, characteristic of old stellar populations in galaxies devoid of ISM. This indicates that the ISM is concentrated near the center.

4.1. *Trends in Line Strengths in Early-Type Galaxies*

The [C II] line strengths of normal spiral and irregular galaxies follow well-defined trends with far-infrared colors [F_ν(60 μm)/F_ν(100 μm)] indicating dependence on dust temperature, and therefore on dust heating radiation density, and on star formation activity, measured by the ratio of far-infrared and blue-band luminosity, $L_{\rm FIR}/L_B$. The ratio $L_{\rm [C\ II]}/L_{\rm FIR}$ decreases dramatically with increasing F_ν(60 μm)/F_ν(100 μm) and $L_{\rm FIR}/L_B$ (Malhotra et al. 1997, 2000).

While [C II] and [O I] are the main coolants of warm ($\simeq$90 K) neutral gas, the main source of heating is the photoejected electrons from dust grains (Watson 1972). Only UV light is effective in producing photoejected electrons since the potential barrier for neutral grains is approximately 6 eV, or more if the grains are positively charged (Bakes & Tielens 1994). The far-infrared continuum reflects the cooling, and thus the total heating, of the dust grains. For galaxies with the most active star formation and warm dust and hence most intense radiation fields, the dust grains become positively charged making the photoelectric heating less efficient. Therefore, we see a decrease in [C II] and [O I] line strengths relative to the dust continuum for the most active galaxies with higher F_ν(60 μm)/F_ν(100 μm) and $L_{\rm FIR}/L_B$ (Fig. 5).

On the other extreme, for galaxies with low rates of current star formation, and softer radiation field, a low $L_{\rm [C\ II]}/L_{\rm FIR}$ is expected since only the UV photons ($\lambda < 2000$ Å) contribute to photoelectric heating of gas, while dust is heated by optical as well as UV photons. In early-type galaxies, which typically have lower active star formation rates relative to the total blue luminosity, we do see a lower $L_{\rm [C\ II]}/L_{\rm FIR}$.

In Figures 5*a* and 5*b* we plot these trends for the whole sample of distant galaxies with the early-type galaxies circled. It is apparent in these figures that the four Es and S0s lie within the broad correlation between $L_{\rm [C\ II]}/L_{\rm FIR}$ and F_ν(60 μm)/F_ν(100 μm) and $L_{\rm FIR}/L_B$. NGC 6958 and NGC

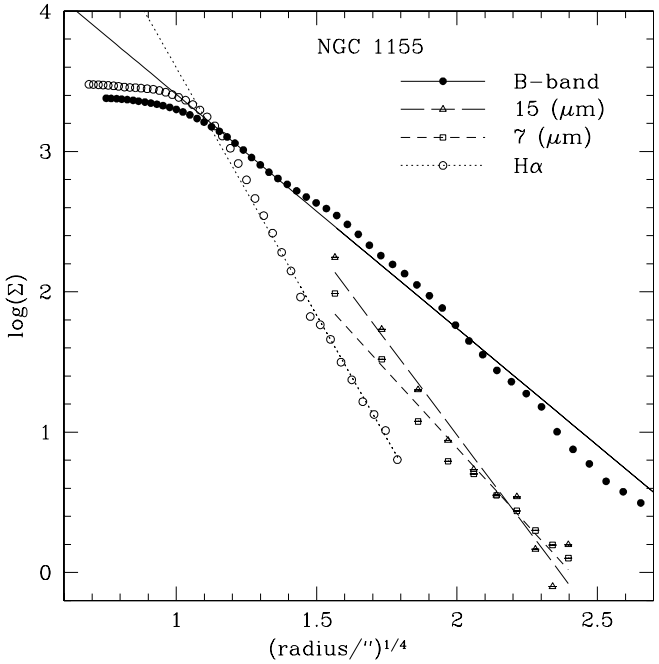

FIG. 4.—Radial profile of optical *B*-band emission (*filled circles*), the Hα emission (*open circles*), and the mid-infrared emission (7 μm: *open squares*; 15 μm: *triangles*) in NGC 1155 is plotted along with the best-fit de Vaucouleurs profile for each wavelength. The mid-infrared light shows a radial distribution intermediate to the *B* band and the Hα.

1052 and NGC 5866 lie at the low end of $L_{\rm FIR}/L_B$, indicating a low rate of current star formation and low extinction. The $L_{\rm [C\,II]}/L_{\rm FIR}$ ratio turns down slightly at the low end of star formation.

4.2. *Origin of* [C II]

The [C II] emission could be from ionized gas in dense H II regions, diffuse ionized gas, neutral atomic medium, or UV-irradiated surfaces of molecular clouds. In nuclear regions of galaxies [C II] arises mostly from dense photodissociation regions (PDRs) (Stacey et al. 1991; Crawford et al. 1985). However, integrated over the disks of normal spiral galaxies, a significant fraction (up to 50%) may also arise from diffuse medium, i.e., the cold neutral medium (Madden et al. 1993) or from extended, low-density ionized gas (Heiles 1994). With the limited knowledge of the phases of the ISM in these galaxies and without assuming that the temperature and density in these phases is very similar to the Galactic values, it is hard to identify the phase of the ISM which produces most of the [C II] emission.

We can rule out H II regions as sources of much [C II]. Assuming case B recombination and $T_e = 10^4$ K, one can place an upper limit on [C II] emission from H II regions (Malhotra et al. 2000) as

$$\frac{L_{\rm [C\,II]}}{L_{\rm H\alpha}} < 5.4 \times 10^4 x_{\rm C}\left(\frac{1}{n_e + 17}\right), \quad (1)$$

where $x_{\rm C}$ is the gas-phase abundance of carbon with respect to hydrogen and n_e is the density of electrons in the H II region in $\rm cm^{-3}$. The inequality sign is due to the fact that not all of the C in H II regions exists as C^+; some will be in the form of C^{2+}.

For low electron density ($n_e \to 0$),

$$\frac{L_{\rm [C\,II]}}{L_{\rm H\alpha}} < 0.33 x_{-4}\,, \quad (2)$$

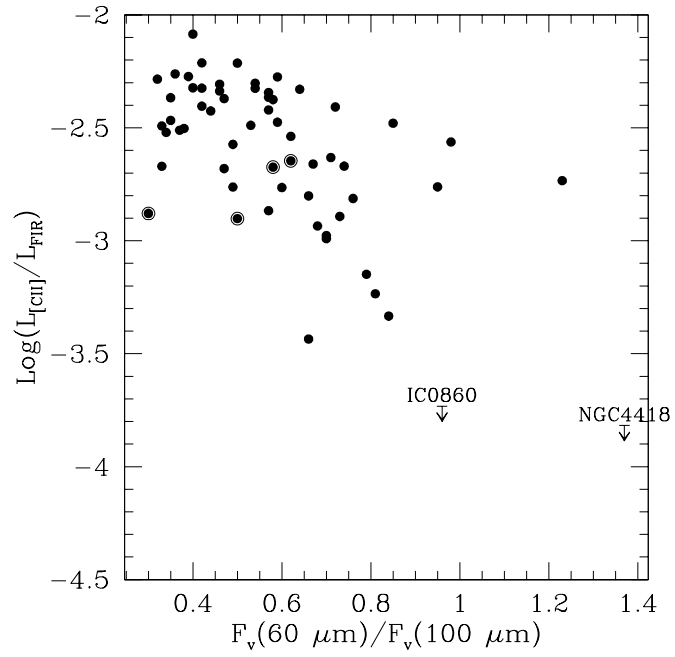

FIG. 5*a*

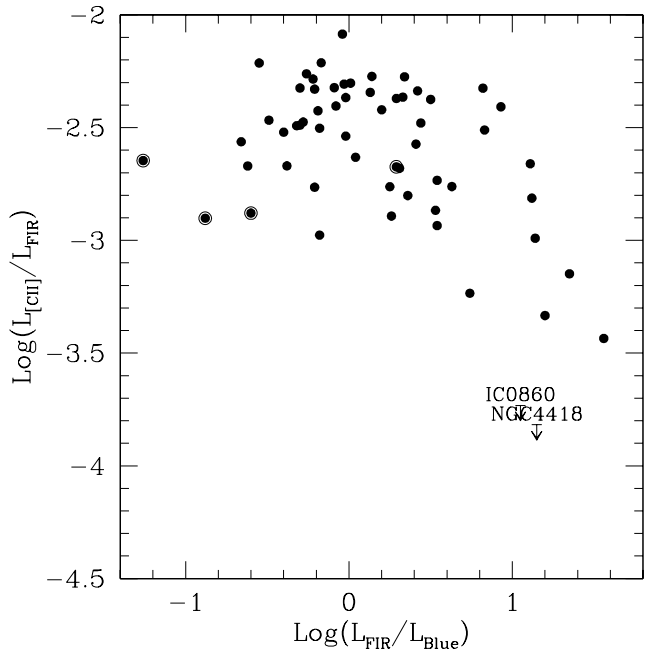

FIG. 5*b*

FIG. 5.—(*a*) Ratio of FIR and [C II] line luminosities is plotted against the dust temperature characterized by the ratio of flux densities at 60 and 100 μm from *IRAS* measurements for a sample of galaxies spanning a whole range of morphologies (cf. Malhotra et al. 2000). The four early-type galaxies are shown with the bull's-eye symbol and lie within the broad trend of decreasing $L_{\rm [C\,II]}/L_{\rm FIR}$ with the increase in $F_\nu(60\ \mu m)/F_\nu(100\ \mu m)$. (*b*) $L_{\rm [C\,II]}/L_{\rm FIR}$ shows a similar trend with the ratio of FIR/blue luminosity, which can be used as an indicator of star formation activity. Three out of four early-type galaxies are at the lower end of mass-normalized star formation activity. These galaxies—NGC 1052, NGC 6958, and NGC 5866—show a lower $L_{\rm [C\,II]}/L_{\rm FIR}$ due to softer radiation field from aging stellar populations.

where $x_{-4} = x_C/10^{-4}$. In the high-density limit ($n_e \gg 17$ cm^{-3}),

$$\frac{L_{[\mathrm{C\,II}]}}{L_{\mathrm{H}\alpha}} < 0.054 x_{-4} \left(\frac{10^2 \text{ cm}^{-3}}{n_e} \right). \quad (3)$$

For NGC 1155, NGC 5866, and NGC 6958 the ratio $L_{[\mathrm{C\,II}]}/L_{\mathrm{H}\alpha}$ is measured to be 2.5, 0.5, and 58, respectively, indicating that most of the [C II] is not associated with H II regions. For NGC 1052 the observed $L_{[\mathrm{C\,II}]}/L_{\mathrm{H}\alpha} = 0.16$. Taking $n_e = 10^3$ cm^{-3}, inferred from the ratio of S II lines (Kim 1989), the contribution of H II regions to [C II] emission is expected to be $L_{[\mathrm{C\,II}]}/L_{\mathrm{H}\alpha} < 0.015$ (for $x_{-4} = 3$), an order of magnitude lower than the observed levels. Thus, it appears that not much of [C II] emission arises from the ionized gas in early-type galaxies. The total extinction is low, so the Hα flux is unlikely to be extincted by more than a factor of 2.

Could the [C II] emission be coming from diffuse H I? It is hard to answer this question given that H I column density has been measured only in NGC 1052. For a cold neutral medium with typical Galactic values $T = 80$ K and $n_{\mathrm{H}} = 90$ cm^{-3}, $M(\mathrm{H\,I})/L_{[\mathrm{C\,II}]} = 20(3 \times 10^{-4}/X_{\mathrm{C}^+})\ M_\odot/L_\odot$. For NGC 1052 $M(\mathrm{H\,I})/L_{[\mathrm{C\,II}]} = 14$ which can easily be accommodated with a slightly higher gas density or warmer gas or some contribution to [C II] from molecular medium. It is quite likely that most of the [C II] emission is associated with molecular gas in NGC 5866, given that the upper limits on H I mass are 10 times lower than the observed $M(\mathrm{H_2})$. Unfortunately, no useful constraints can be placed on the origin of [C II] in NGC 1155 and NGC 6958 where neither H I nor CO have been detected. It should be easy to estimate the H I contribution to the origin of [C II] emission in NGC 1155 with H I observations. If [C II] is associated with H I, we should see $M(\mathrm{H\,I}) \simeq 10^8\ M_\odot$.

4.3. [C II]/CO *Ratio*

For [C II] emission arising from photodissociation regions softer radiation leads to a lower fraction of gas in C^+ due to reduced photodissociation of CO molecules, making a thinner C^+ layer on the surface of the molecular cloud (Spaans et al. 1994). This scenario predicts a lower ratio of the flux in [C II] versus various CO transitions as well as lower $L_{[\mathrm{C\,II}]}/L_{\mathrm{FIR}}$. For Galactic H II and OB star-forming regions and for starburst galaxies, the ratio $L_{[\mathrm{C\,II}]}/L_{\mathrm{CO}}(1\text{–}0) = 4100$, whereas for more quiescent spiral galaxies this ratio was found to be $L_{[\mathrm{C\,II}]}/L_{\mathrm{CO}}(1\text{–}0) = 1500$ (Stacey et al. 1991). For NGC 5866, which is the only galaxy in the current sample with a CO measurement, $L_{[\mathrm{C\,II}]}/L_{\mathrm{CO}}(1\text{–}0) \leq 570$. This is an upper limit because the CO is measured in the 45″ beam of FCRAO (Thronson et al. 1989) and the [C II] is measured in a 70″ beam. This provides evidence for a soft radiation field. For NGC 6958 and NGC 1052, we have only upper limits on CO(1–0) emission. For NGC 1052 $L_{[\mathrm{C\,II}]}/L_{\mathrm{CO}}(1\text{–}0) > 1100$, which is comparable to the quiescent spiral galaxy sample, but most of the [C II] seems to be associated with the atomic gas in this galaxy, while the low $L_{[\mathrm{C\,II}]}/L_{\mathrm{CO}}(1\text{–}0)$ prediction in soft radiation fields is made for dense PDRs on the surfaces on molecular clouds. In NGC 5866, where we find low $L_{[\mathrm{C\,II}]}/L_{\mathrm{CO}}(1\text{–}0)$ values, the $M(\mathrm{H\,I})/M(\mathrm{H_2}) < 0.1$ indicating that most of the [C II] is associated with molecular clouds, providing a cleaner diagnostic of the softer radiation field. For NGC 6958 upper limits on CO imply $L_{[\mathrm{C\,II}]}/L_{\mathrm{CO}}(1\text{–}0) > 170$, and more sensitive CO observations are needed.

4.4. *Physical Conditions in the Gas*

With the few FIR line measurements of these galaxies, we can attempt to derive the physical conditions in the warm, neutral, FIR-emitting gas.

NGC 1155.—We compare the two FIR line ([C II] and [O I] (63 μm)) and line-to-continuum ratios in NGC 1155 to models of photodissociation regions by Kaufman et al. (1999). Using the ratios ([C II] + [O I])/FIR and [O I]/[C II] gives density $n \simeq 10^{3.7}$ cm^{-3} and FUV flux $G_0 \simeq 10^{3.3}$ (Malhotra et al. 2000) (G_0 conventionally is the FUV flux normalized to the average local interstellar flux of 1.6×10^{-3} ergs cm^{-2} s^{-1}; Habing 1968). There are no H I or CO measurements for this galaxy. The chances of detecting both are excellent, both because of the high minimum mass of hydrogen associated with the C^+ emission and because of the density of the gas derived.

NGC 1052.—The column density of H I is measured to be 2.5×10^{20} cm^{-2} (van Gorkom et al. 1986) near the nucleus and about 1′ away. It is then reasonable to assume that $N(\mathrm{H}')$ is constant in the LWS 70″ beam and the [C II]-emitting gas fills the beam: $I([\mathrm{C\,II}]) = 1.1 \times 10^{-6}$ ergs cm^{-2} s^{-1} sr^{-1}. Using this in the following equation with the further assumptions that the temperature of the gas $T > 91$ K and the ionization fraction is small ($X_e < 10^{-3}$, so we can neglect collisional excitation due to electrons), we can solve for the density of the gas n_{H}:

$$I([\mathrm{C\,II}]) = 2.3 \times 10^{-21} N(\mathrm{H\,I}) X_{\mathrm{C}^+} \times \left(\frac{2e^{(-91/T)}}{1 + 2e^{(-91/T)} + n_{\mathrm{crit}}/n_{\mathrm{H}}} \right), \quad (4)$$

where $n_{\mathrm{crit}} = 2 \times 10^3$ is the critical density for collisions with H I (Launay & Roeff 1977; Hayes & Nussbaumer 1984) and X_{C^+} (the C^+ abundance) is taken to be the Galactic value of 1.4×10^{-4}. The density of the H I then is derived to be $n_{\mathrm{H}} = 14$ cm^{-3}, consistent with [C II] arising from diffuse H I.

NGC 5866.—Comparing the models to the observed ([C II] + [O I])/FIR, [C II]/[O I], and [C II]/CO(1–0) ratios does not yield a solution for gas and radiation density in NGC 5866 because the models assume a harder radiation field and that half the dust heating is from far-UV. In softer radiation fields from old stars, the optical light contributes a larger fraction of the dust heating and therefore to the FIR continuum.

Ignoring ([C II] + [O I])/FIR ratio, we estimate the intensity of [C II] emission in the beam, assuming a beam filling factor of 1, to be $I([\mathrm{C\,II}]) = 5.5 \times 10^{-6}$ ergs cm^{-2} s^{-1} sr^{-1}. Using this and the ratios [O I]/[C II] = 0.2 and [C II]/CO(1–0) ≤ 570, PDR models of Kaufman et al. (1999) give the density $n = 3 \times 10^3$ cm^{-3} and UV radiation density $G_0 = 1$–3. The same models estimate a temperature of about 30–40 K at the surface of the molecular clouds and a thermal pressure of $\simeq 10^5$ K cm^{-3}, which is 30 times higher than the local solar neighborhood value but 10 times lower than the pressure at the center regions of the Milky Way (10^6 K cm^{-3}; Spergel & Blitz 1992). This is plausible, since the LWS beam encompasses gas at radius less than 2 kpc from the center of NGC 5866. The PDR models then overpredict ([C II] + [O I])/FIR = 5×10^{-3}, when the observed ([C II] + [O I])/FIR = 2×10^{-3}. The PDR models assume that equal amounts of heating of the dust come from UV and non-UV photons. The current discrepancy in ([C II] + [O I])/FIR ratio thus implies that 4 times

as much heating of the dust grains comes from non-UV radiation as from UV. This is also our favored scenario for the observed low $L_{[C\,II]}/L_{FIR}$ and $L_{[C\,II]}/L_{CO}(1–0)$.

4.5. *Gas Energetics*

In spiral galaxies [C II] is frequently used as a measure of star formation activity (Stacey et al. 1991). In early-type galaxies emission in the fine-structure lines [C II] and [O I] do not necessarily indicate current star formation (or PDR emission). In spirals, [C II] and [O I] are the major coolant of warm neutral gas and most of the heating is by photoelectrons from dust grains (Watson 1972). The potential barrier to photoejection from neutral grains is approximately 6 eV (Bakes & Tielens 1994), or higher if the grains are positively charged. This means that only photons shortward of $\sim$2000 Å contribute to heating of the gas. Old stellar populations (planetary nebulae and horizontal-branch and post–asymptotic giant branch stars) in Es/S0s produce enough ionizing flux shortward of 912 Å to explain the Hα emission seen (Rose & Tinsley 1974; Binette et al. 1994).[10] So it is possible that they contribute to heating the gas by photoelectric heating. But what is the magnitude of that contribution?

To answer that question we estimate photoelectric gas heating by UV photons from old stellar populations. We use GISSEL (Bruzual & Charlot 1993) stellar population models of instantaneous burst of ages 10 and 13 Gyr to calculate the UV spectra of early-type galaxies. The mass of each galaxy is normalized to match the *B*-band flux within the LWS beam of 70″. An upper limit to the gas-heating rate is calculated by assuming that the work function of the grains is 6 eV and the yield of photoelectrons heating process is $\gamma = 0.1$ (Tielens & Hollenbach 1985). This is an upper limit on the heating and a lower limit on the UV required because it neglects the positive charging of the grains by photoelectric process, which raises the potential barrier for ejecting electrons off grains, therefore requiring even more energetic photons. We neglect here the contribution of negatively charged grains, which have an ionization potential as low as 2 eV, because they are estimated to contribute less than 10% of the heating (Spaans et al. 1994). The total power that goes into heating the gas is given by

$$L_{PE} = \gamma f_{abs} \int (h\nu - 6\ \mathrm{eV}) N_\nu\, d\nu\ . \qquad (5)$$

[10] If the ionizing photons come from old stellar populations, one might expect the Hα distribution to be diffusely distributed, but it is usually seen to be associated with dust lanes (Goudfrooij et al. 1994a).

In the above equation N_ν is the number of photons at frequency ν and f_{abs} is the fraction of photons absorbed by the dust. The value of f_{abs} should be less than unity given the low ratio of ISM to stars; f_{abs} is estimated from the observed values of L_B/L_{FIR} and using a standard extinction curve with the spectral energy distribution from stellar population models. We note here in passing that it was not possible to reproduce the high $L_{FIR}/L_B = 0.29$ seen in NGC 1155 with any of the old population models by any extinction values. For the other three galaxies A_V varied from 0.05 to 0.25. Table 2 lists the heating luminosity L_{PE} from old stellar populations, compared to the luminosity of the [C II] and [O I] lines; for NGC 1052 and NGC 6958 the [O I] line strength is estimated using the correlation between [O I]/[C II] and $F_\nu(60\ \mu m)/F_\nu(100\ \mu m)$ (Malhotra et al. 2000).

The UV heating produced by the old stellar populations fails to account for the [C II] and [O I] emission by factors of 2 or 3 in NGC 1052, NGC 6958, and NGC 5866 and clearly fails for NGC 1155 by a factor of about 20. The theoretical estimates of UV production by old populations are uncertain and vary significantly with age and metallicity (cf. Magris & Bruzual 1993). Therefore, a factor of 2–3 discrepancy in the required UV and theoretical UV production does not necessarily imply the presence of extra UV sources. However, for NGC 1155 we can conclude that the strength of [C II] and [O I] emission implies a higher UV production than can be explained by the old populations.

This conclusion is also supported by the optical spectrum of NGC 1155, which shows narrow emission lines. The ratio of [N II] λ6583/Hα $\simeq$ 0.5 characteristic of H II regions (Fig. 6). NGC 5866 shows a ratio of [N II] λ6583/Hα $\simeq$ 1.34, and Ho, Fillipenko, & Sargent (1997) classify the nucleus as a transition object between a LINER and an H II nucleus.

The observed far-UV–optical colors $(1550 - V)$ of Es/S0s vary by a factor of 10 for active and quiescent galaxies (Brown et al. 1998; Burstein et al. 1988, hereafter B3FL). The scatter is reduced by using a correlation with the magnesium index Mg_2. Quiescent E/S0 galaxies, with or without an active nucleus, show a higher Mg_2 index than galaxies with star formation, except when they have very red $(1550 - V)$ colors. We compare our sample to B3FL's Figure 1*a*, except we estimate the flux in the 1500 Å band from the UV required to produce the [C II] and [O I] line emission (hereafter referred to as $FUV_{[C\,II]}$), since three out of four galaxies (except NGC 1052) do not have their far-UV measured. We cannot comment on NGC 1155 whose V and Mg_2 measurements are not available. NGC 6958 and NGC 5866 have low Mg_2 indices, 0.23 and 0.21, respectively (Davies et al. 1987; Huchra et al. 1996; Fisher,

TABLE 2

LUMINOSITIES IN COOLING LINES COMPARED TO PHOTOELECTRIC HEATING

Name	L[C II][a]	L([O I])[a]	L([C II]+[O I]) ($10^6\ L_\odot$)	L(Hα) ($10^6\ L_\odot$)	L_{PE} (10 Gyr) ($10^6\ L_\odot$)	L_{PE} (13 Gyr)
NGC 1052.....	0.5	(0.25)[b]	0.75	3.2	0.11	0.36
NGC 1155.....	20	20	40	8.1	0.85	2.80
NGC 5866.....	2	0.5	2.5	4.2	0.24	0.78
NGC 6958.....	1.6	(0.66)[b]	2.3	0.025	0.46	1.58

[a] Fluxes in the [O I] (63 μm) and [C II] lines are taken from Malhotra et al. 2000; typical uncertainty in a line flux is 30%.

[b] [O I] (63 μm) flux is derived from the [C II] flux and the *IRAS* colors $F_\nu(60)/F_\nu(100)$ using the correlation seen between [O I]/[C II] and $F_\nu(60)/F_\nu(100)$ (Malhotra et al. 2000).

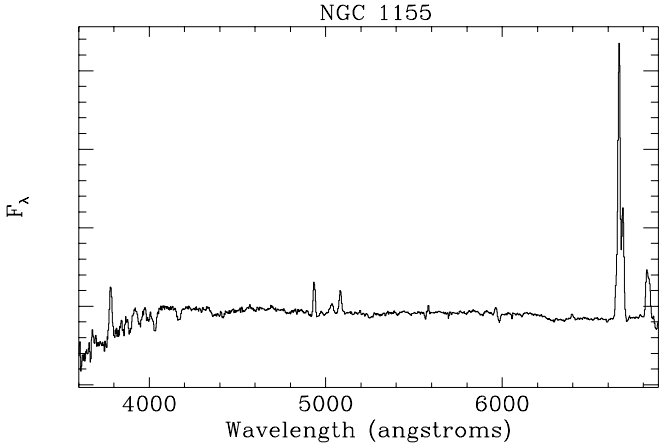

FIG. 6.—Optical spectrum on NGC 1155 shows narrow lines and line ratios characteristic of H II regions, i.e., Hα/[N II] > 1), lending support to our conclusion from the analysis of FIR lines that there has been recent star formation.

Franx, & Illingworth 1996). NGC 5866 has normal $FUV_{[C\,II]} - V$ color, so the low Mg_2 could be due to recent star formation or due to extinction by the central dust lane (Fisher et al. 1996). NGC 6958 has red color $FUV_{[C\,II]} - V = 4.2$, and lies on the locus of quiescent galaxies with red colors and low Mg_2 indices, indicating little recent star formation. For NGC 1052 the $FUV_{[C\,II]} - V = 1.08$ mag, 2 mag bluer than the *IUE* observed color (B3FL). In other words, from the [C II] estimate NGC 1052 is bluer than the sample of quiescent galaxies. The $FUV_{[C\,II]}$ is also 6 times higher than the observed UV in this galaxy, although some uncertainty remains because *IUE* measured fluxes between 1300 and 3000 Å and $FUV_{[C\,II]}$ is an estimate of flux between 912 and 2070 Å. The extra UV in NGC 1052 could come from very obscured source(s), either star formation or the central AGN.

Other sources of gas heating include X-rays from hot gas and active nuclei. Only NGC 1052 shows evidence for a Seyfert nucleus and is detected in X-rays by *Einstein* and *ROSAT*. It shows a higher luminosity in X-rays than the average L_X-L_B relation (Fabbiano, Kim, & Trinchieri 1992), and the X-ray gas temperature is much higher than expected from the average relation between stellar velocity dispersion and temperature of the X-ray gas, indicating that X-ray emission is dominated by AGN or X-ray binaries rather than diffuse hot gas (Davis & White 1996). The X-ray luminosity of NGC 1052 is $\simeq 3 \times 10^6\ L_\odot$. About 10% of X-ray luminosity could be used for gas heating in atomic medium and about 40% in molecular medium in the so-called X-ray dissociation regions (XDRs) (Maloney, Hollenbach, & Tielens 1996). In NGC 1052 X-rays could make a significant contribution to gas heating. But in XDRs one expects a higher line-to-continuum ratio for the [C II] and [O I] lines because the X-rays are equally efficient at heating the gas and the dust, whereas the UV radiation in PDRs heats dust much more efficiently. Because NGC 1052 shows a lower $L_{[C\,II]}/L_{FIR}$ than the average for other (mostly spiral) galaxies in the sample, a significant X-ray heating of the cool gas seems unlikely. NGC 1155 and NGC 6958 were not detected by *Einstein* or *ROSAT* all-sky survey. We estimate the X-ray luminosity from the L_X-L_B relation (Fabbiano et al. 1992) to be $\simeq 10^5$ and $\simeq 0.7 \times 10^5\ L_\odot$ for NGC 6958 and NGC 1155, respectively. That is simply not sufficient to heat the gas to produce the [C II] flux seen (Table 2). NGC 5866 has a luminosity of $L_X(N5866) = 0.7 \times 10^5\ L_\odot$, again insufficient to heat the cool gas enough to explain the flux in the far-infrared cooling lines.

5. SUMMARY AND CONCLUSIONS

From observations of two elliptical galaxies and two S0s with ISOCAM and *ISO* LWS we can conclude the following:

1. The mid-infrared emission from early-type galaxies arises both from ISM and photospheres of stars. The 7 μm/15 μm ratio varies with radius indicating that ISM dominates at the centers and in NGC 6958 is not very extended. In NGC 1155 the dust emission extends to 10 kpc. In NGC 1052 the Seyfert nucleus dominates the mid-IR emission. In NGC 5866, the mid-IR emission at 7 and 15 μm follows the central dust lane.

2. [C II] (158 μm) and [O I] (63 μm) lines are detected in galaxies where H I and CO detections were difficult, making *ISO* LWS one of the sensitive probes of small quantities of cool ISM ($T \sim 100$ K). [C II] is not mostly from classical H II regions. [C II] emission is associated with H I in NGC 1052 and with molecular gas in NGC 5866.

3. The line-to-continuum ratio $L_{[C\,II]}/L_{FIR}$ measures the efficiency of gas heating by photoelectric heating. In three of the four early-type galaxies considered here, $L_{[C\,II]}/L_{FIR}$ is lower by a factor of 2–5 than the typical values in a sample of 60 normal galaxies. A softer radiation field, i.e., relatively deficient in UV, is the most likely explanation. This is corroborated by a low $L_{[C\,II]}/L_{CO}(1–0)$ ratio observed in NGC 5866.

4. The fluxes in the cooling lines, [C II] and [O I], provide fairly stringent lower limits on the UV flux between 912 and 2100 Å. With all the uncertainties in modeling, UV from evolved stellar populations is insufficient by a factor of 2–3 for NGC 1052, NGC 5866, and NGC 6958 and a clear factor of 20 for NGC 1155. Heating of cool ISM by X-rays is a plausible scenario only for NGC 1052. In NGC 6958, NGC 1052, and NGC 5866, it is plausible that old stars produce enough UV to heat the ISM to explain the cooling by [C II] line. In NGC 1155, young stars are needed to provide the UV heating to account for the cooling via the FIR lines.

5. Comparing the [C II] and [O I] (63 μm) line flux measurements of NGC 1155 with PDR models by Kaufman et al. (1999), we infer gas density $n \simeq 10^2\ cm^{-3}$ and UV radiation density $\simeq 10^2 G_0$, where G_0 is the UV radiation density in the solar neighborhood. Comparing the models to the observed [C II], [O I], and CO(1–0) line ratios for NGC 5866 yields $G_0 = 1–3$ and $n = 3 \times 10^3\ cm^{-3}$ and the estimate that non-UV radiation contributes about 80% of the dust heating in this galaxy.

We thank Michael Kaufman, Harry Ferguson, Sue Madden, John Mulchaey, Jill Knapp, and James Rhoads for helpful discussions. We also thank the anonymous referee and the scientific editor for many suggestions that improved the paper. This research has made use of the NASA/IPAC Extragalactic Database (NED) which is operated by the JPL, California Institute of Technology, under contract with NASA. This work was supported by *ISO* data

analysis funding from NASA and carried out at IPAC and the JPL of the California Institute of Technology. S. M.'s research is supported by a Hubble Fellowship grant HF-01111.01-98A from the Space Telescope Science Institute, which is operated by the Association of Universities for Research in Astronomy, Inc., under NASA contract NAS 5-26555. *ISO* is an ESA project with instruments funded by ESA Member States (especially the PI countries: France, Germany, the Netherlands, and the United Kingdom) and with the participation of ISAS and NASA.

REFERENCES

Bakes, E. L. O., & Tielens, A. G. G. M. 1994, ApJ, 427, 822
Binette, L., Magris, C. G., Stasinska, G., & Bruzual, A. G. 1994, A&A, 292, 13
Brown, T. M., Ferguson, H. C., Deharveng, J.-M., & Jedrzejewski, R. I. 1998, ApJ, 508, L139
Bruzual, A. G., & Charlot, S. 1993, ApJ, 405, 538
Burstein, D., Bertola, F., Buson, L. M., Faber, S. M., & Lauer, T. R. 1988, ApJ, 328, 440 (B3FL)
Cesarsky, C. J., et al. 1996, A&A, 315, L32
Clegg, P. E., et al. 1996, A&A, 315, L38
Crawford, M. K., Genzel, R., Townes, C. H., & Watson, D. M. 1985, ApJ, 291, 755
Dale, D. A., et al. 2000, AJ, 120, 583
Davies, R. L., et al. 1987, ApJS, 64, 581
Davis, D. S., & White, R. 1996, ApJ, 470, L35
Fabbiano, G., Kim, D.-W., & Trinchieri, G. 1992, ApJS, 80, 531
Fisher, D., Franx, M., & Illingworth, G. 1996, ApJ, 459, 110
Fosbury, R. A. E., Mebold, U., Goss, W. M., & Dopita, M. A. 1978, MNRAS, 183, 549
Goudfrooij, P., Hansen, L., Jorgensen, H. E., & Norgaard-Nielsen, H. U. 1994a, A&AS, 105, 341
Goudfrooij, P., Hansen, L., Jorgensen, H. E., Norgaard-Nielsen, H. U., De Jong, T., & Van Den Hoek, L. B. 1994b, A&AS, 104, 179
Habing, H. 1968, Bull. Astron. Inst. Netherlands, 19, 421
Hayes, M. A., & Nussbaumer, H. 1984, A&A, 134, 193
Haynes, M. P., Herter, T., Barton, A. S., & Benensohn, J. S. 1990, AJ, 99, 1740
Heiles, C. 1994, ApJ, 436, 720
Helou, G. 1986, ApJ, 311, L33
Helou, G., et al. 1996, A&A, 315, L157
Helou, G., Khan, I., Malek, L., & Boehmer, L. 1988, ApJS, 68, 151
Ho, L. C., Fillipenko, A. V., & Sargent, W. L. W. 1997, ApJS, 112, 315
Hollenbach, D. J., & Tielens, A. G. G. M. 1997, ARA&A, 35, 179
———. 1999, Rev. Mod. Phys., 71, 173
Hollenbach, D. J., Tielens, A. G. G. M., & Takahashi, T. 1991, ApJ, 377, 192
Huchra, J. P., Brodie, J. P., Caldwell, N., Christian, C., & Schommer, R. 1996, ApJS, 102, 29
Jura, M., Kim, D. W., Knapp, G. R., & Guhathakurta, P. 1987, ApJ, 312, L11
Kaufman, M. J., Wolfire, M. G., Hollenbach, D. J., & Luhman, M. L. 1999, ApJ, 527, 795
Kessler, M. F., et al. 1996, A&A, 315, L27
Kim, D. W. 1989, ApJ, 346, 653
Knapp, G. R., Guhathakurta, P., Kim, D. W., & Jura, M. 1989, ApJS, 70, 329
Knapp, G. R., Gunn, J. E., & Wynn-Williams, C. G. 1992, ApJ, 399, 76
Knapp, G. R., & Rupen, M. P. 1996, ApJ, 460, 271
Knapp, G. R., Rupen, M. P., Fich, M., Harper, D. A., & Wynn-Williams, C. G. 1996, A&A, 315, L75
Launay, J. M., & Roueff, E. 1977, A&A, 56, 289
Lees, J. F., Knapp, G. R., Rupen, M. P., & Phillips, T. G. 1991, ApJ, 379, 177
Lemke, D., et al. 1996, A&A, 315, L64
Madden, S. C., Geis, N., Genzel, R., Herrmann, F., Jackson, J., Poglitsch, A., Stacey, G. J., & Townes, C. H. 1993, ApJ, 407, 579
Madden, S. C., Vigroux, L., & Sauvage, M. 1997, Extragalactic Astronomy in the Infrared, ed. G. A. Mamon, T. X. Thuan, & J. T. V. Tran (Paris: Editions Frontières), 229
Magris, C. G., & Bruzual, A. G. 1993, ApJ, 417, 102
Malhotra, S., et al. 1996, A&A, 315, L161
———. 1997, ApJ, 491, L27
———. 2000, ApJ, submitted
Maloney, P. R., Hollenbach, D. J., & Tielens, A. G. G. M. 1996, ApJ, 466, 561
Phillips, M. M., Jenkins, C. R., Dopita, M. A., Sadler, E. M., & Binette, L. 1986, AJ, 91, 1062
Plana, H., & Boulesteix, J. 1996, A&A, 307, 391
Plana, H., Boulesteix, J., Amram, P., Carignan, C., & Mendes De Oliveira, C. 1998, A&AS, 128, 75
Puget, J. L., & Leger, A. 1989, ARA&A, 27, 161
Roberts, M. S., Hogg, D. E., Bregman, J. N., Forman, W. R., & Jones, C. 1991, ApJS, 75, 751
Rose, W. K., & Tinsley, B. M. 1974, ApJ, 190, 243
Rupen, M. 1997, in ASP Conf. Ser. 116, The Nature of Elliptical Galaxies, ed. M. Arnaboldi, G. S. Da Costa, & P. Saha (San Francisco: ASP), 322
Sadler, E. M., & Gerhard, O. E. 1985, MNRAS, 214, 177
Sauvage, M., & Thuan, T. X. 1994, ApJ, 429, 153
Spaans, M., Tielens, A., Van Dishoeck, E., & Bakes, E. 1994, ApJ, 437, 270
Spergel, D. N., & Blitz, L. 1992, Nature, 357, 665
Stacey, G. J., Geis, N., Genzel, R., Lugten, J. B., Poglitsch, A., Sternberg, A., & Townes, C. H. 1991, ApJ, 373, 423
Thronson, H. A., Jr., Tacconi, L., Kenney, J., Greenhouse, M. A., Margulis, M., Tacconi-Garman, L., & Young, J. S. 1989, ApJ, 344, 747
Tielens, A. G. G. M., & Hollenbach, D. 1985, ApJ, 291, 722
van Gorkom, J. H., & Schiminovich, D. 1997, in ASP Conf. Ser. 116, The Nature of Elliptical Galaxies, ed. M. Arnaboldi, G. S. Da Costa, & P. Saha (San Francisco: ASP), 310
van Gorkom, J. H., Knapp, G. R., Raimond, E., Faber, S. M., & Gallagher, J. S. 1986, AJ, 91, 791
Vigroux, L., et al. 1999, in Universe as Seen by *ISO*, ed. P. Cox & M. F. Kessler (ESA SP-427; Noordwijk: ESA), 805
Walsh, D. E. P., van Gorkom, J. H., Bies, W. E., Katz, N., Knapp, G. R., & Wallington, S. 1990, ApJ, 352, 532
Watson, W. D. 1972, ApJ, 176, 103
Wiklind, T., Combes, F., & Henkel, C. 1995, A&A, 297, 643